Investigation of heat exchange processes in the lining of induction furnaces

Tokhir Tursunov*, *Nodirjon* Tursunov , and *Talgat* Urazbayev

Tashkent State Transport University, Tashkent, Uzbekistan

Abstract. This paper discusses scientific research in the direction of energy saving and the efficiency of heat transfer processes. In this direction, in particular, in the optimization of the design and modernization of heat exchange processes, as well as in the development of energy and resource-saving technologies, it is necessary to reconsider the lining thickness of induction melting furnaces.

The research on the optimization the thickness of the lining, consists of thermodynamic and thermal processes taking place in the liquid metal bath and on the boundaries of the refractory layer of the lining. The power of heat loss through the lining of a cylindrical wall is complex heat transfer under boundary conditions of the first and third kind. Beside that the active power lost in the inductor, the power released in the metal and useful power are calculated. This has resulted in an adjustment to the overall efficiency calculation, which includes thermal efficiency and electrical efficiency.

On the basis of thermal and electrical calculations for ICF-6 LMZ with a capacity of 6 tons, the rational thickness of the lining of the crucible wall is equal to $\delta_{\phi} = 0.115 \ldots 0.120\ mm$, which corresponds to the relation $\frac{D_{vt}}{D_m} = 1.23 \ldots 1.26$.

1 Introduction

The study of thermal transfer processes within lining carried out for 6 ton induction crucible furnaces (ICF-6) when smelting steel grade 20GL (analogue for EU=G21Mn5 and USA=A352GrLCC) in the Subsidiary Foundry Mechanical Plant (FMP) in Tashkent.The design parameters of the furnace and its associated parts were used for basic calculations of heat transfer through the furnace lining. In addition, the main characteristics of the furnace operation, determined by the technology of steel smelting, were used. At the moment, in the transport industry there is a need for the production of parts from manganese steels. In particular, from steel grade 20 GL.

Steel 20GL refers to medium-carbon and low-alloy steels, which contain an increased amount of manganese, as well as silicon, chromium, nickel, copper and some other elements (table 1).

*Corresponding author: t.tursunov87@gmail.com

Table 1. Chemical (GOST 977-88) and calculated composition of steel grade 20GL, % (wt.)

C	Mn	Si	S	P	Cr	Ni	Cu
			no more				
0.17…0.25	1.10…1.40	0.30…0.50	0.04	0.04	0.30	0.30	0.30
0.20	1.26	0.42					

Table 2. Mechanical properties at 20°C

Heat treatment	Thermal holding		$\sigma_{0.2}$, MPa	σ_v, MPa	δ_5, %	ψ, %	KC, J/sm^2
	t, °C	τ, h	no more				
Annealing at 900 °C	450	10000	245	490	23	35	39
	500		220	475	26	47	49

On the basis of the electromagnetic wave equation [2], the electrodynamics regularities [2, 3] were determined in the process of melting in induction crucible furnaces, the following equations were identified:

The scalar expression of the complex value of the power flow through the side surface of a metal cylinder with a diameter D_m, numerically equal to the area of the side surface S_{act}, allows us to obtain calculation formulas for the active power P_m (1) released in liquid steel and the reactive power Q_{m} (2) arising in liquid steel:

$$P_m = ReS \cdot S_{act} k_{m\text{P}} \approx 2 \cdot 10^{-6} (IN_1)^2 \pi D_m h_m \sqrt{\rho_m \mu_{rm} f} k_{m\text{P}} \approx \approx 6.28 \cdot 10^{-6} (IN_1)^2 D_m h_m \sqrt{\rho_m f} k_{m\text{P}} = 2.4 \cdot 10^{-7} (IN_1)^2 k_{m\text{P}}, kWt \quad (1)$$

$$Q_{\text{m}} = Im\, S \cdot S_{\text{act}} k_{\text{m}Q} \approx 2 \cdot 10^{-6} (IN_1)^2 \pi D_{\text{m}} h_{\text{m}} \sqrt{\rho_{\text{m}} \mu_{r\text{m}} f} k_{\text{m}Q} \approx \approx 6{,}28 \cdot 10^{-6} (IN_1)^2 D_m h_m \sqrt{\rho_m f} k_{mQ} = 2{,}4 \cdot 10^{-7} (IN_1)^2 k_{mQ}, kVAr. \quad (2)$$

where $\rho_m = 140 \cdot 10^{-8}$ Ohm·m – for liquid steel grade 20GL ($\mu_r = 1$); $S_{\text{act}} = \pi D_m h_m \approx 4.53\, m^2$- the area of the lateral ("active") surface of the heated volume of liquid metal in the ITP crucible with a diameter of $D_{\text{m}} = 1{,}05\, m$ and height $h_{\text{m}} = 1.375\, m$; $2 \cdot 10^{-6} \approx \frac{2\pi \cdot 10^{-6}}{\sqrt{10}}$ – coefficient; $6.28 \cdot 10^{-6} \approx 2\pi \cdot 10^{-6}$ – coefficient; $k_{m\text{P}}, k_{mQ}$ - coefficients of active and reactive power, respectively, taking into account the features of the physical processes of propagation and attenuation of cylindrical electromagnetic waves in the liquid metal ICF-6 and depending on the relative diameter of the cylinder D_m/δ_{ekv} obtained on the basis of calculation [1, 2] (fig.1).

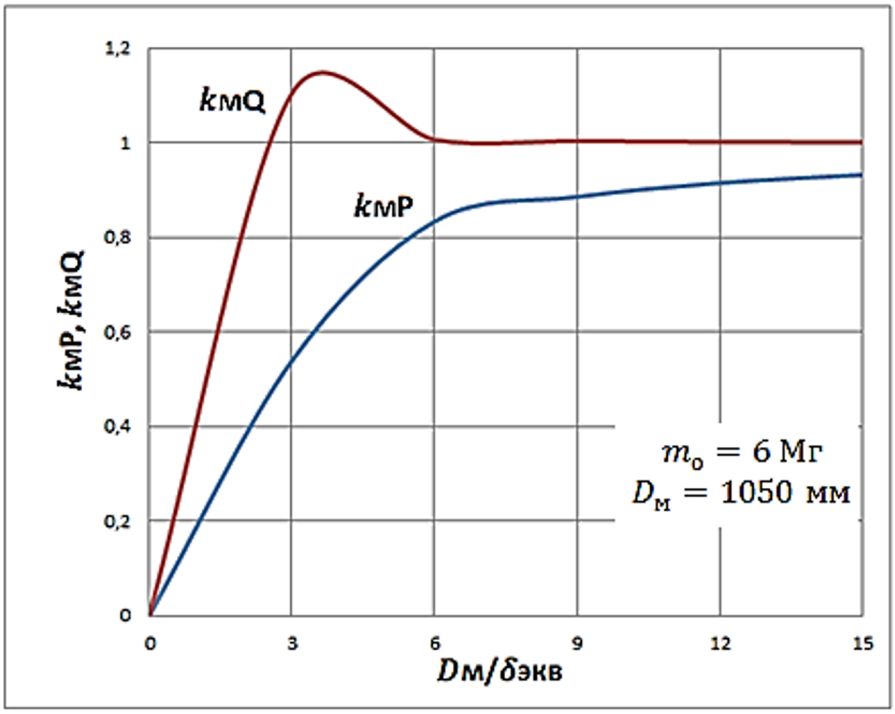

Fig. 1. Curves for determining active and reactive power factors

2 Objects and methods of research

Thermal calculations for the lining of induction furnaces should be carried out taking into account preliminary data [1-5]:

- to define the material of the lining of induction furnaces in steel 20GL (analogue for EU=G21Mn5 and USA=A352GrLCC) [1]. Study with regard of the lining in difficult conditions, such as thermal, corrosive and erosive effects of liquid metal, chemical corrosion of slag, ferrostatic pressure of the liquid metal column. This study was carried out at the 6-ton induction crucible furnace (ICF-6) in the conditions of the Tashkent foundry and mechanical plant. To determine the intensity of the circulation of molten metal throughout the volume of the crucible, which leads to erosion and erosion of the working layer of the lining, the following were determined: electromagnetic force, and specific electromagnetic force applied to a unit volume [2];

- the study of electromagnetic phenomena in the ICF-6 when smelting steel for determining the electromagnetic phenomena in a liquid metal in a crucible to estimate electrical losses and main parameters in an inductor. It is necessary to use the rotor of the magnetic and electric field strengths in cylindrical coordinates for furnaces [2, 3];

- to define magnetic field of a real inductor of ICF-6 during smelting of 20GL [4]. The study of the magnetic field of a real inductor and the fill factor of the inductor needs for enlarging the service life of the lining and increase the number of melts;

- to conduct thermodynamic calculation of complex deoxidation with elements for steel 20GL [5]. operational reliability and increasing the mechanical properties of castings made of 20GL steel in the cost of their manufacture.

- calculation of energy and material balance for ICF-6 [6].

Calculation of the power of heat losses of ICF-6

1. Heat loss through the wall lining

The power of heat loss through the lining of a cylindrical wall is calculated by the formula for complex heat transfer under boundary conditions of the first and third kind:

$$\Phi_w = \frac{\mathrm{T_m} - T_{\mathrm{n_2}0}}{\frac{1}{2\pi\lambda_\mathrm{l} h_m}\ln\frac{D_{\nu\mathrm{т}}}{D_m} + \frac{\delta_\mathrm{c}}{\lambda_\mathrm{c}\cdot S_{\mathrm{p}.c}} + \frac{\delta_{\mathrm{ст}}}{\lambda_{\mathrm{ст}}\cdot S_{\mathrm{p.ст}}} + \frac{1}{\alpha_{\mathrm{c.th}}\cdot S_{\mathrm{c.th}}}}\cdot 10^{-3} \quad (3)$$

2. Heat loss through the bottom lining

The power of heat loss through the lining of the hearth is calculated by the formula for complex heat transfer under boundary conditions of the first and third kind:

$$\Phi_{bot} \approx \frac{\mathrm{T_m} - T_{\mathrm{air}}}{\frac{\delta_{\mathrm{n.l}}}{\lambda_{\mathrm{n.l}}\cdot S_{\mathrm{p}.n.l}} + \frac{\delta_{\mathrm{бет}}}{\lambda_{\mathrm{con}}\cdot S_{\mathrm{p}.con}} + \frac{1}{\alpha_{\mathrm{c.t.h}}\cdot S_{\mathrm{t.h}}}}\cdot 10^{-3} \quad (4)$$

3. Heat loss through the vault:

The power of heat loss through the lining of the vault (roof) is calculated according to the formula of complex heat transfer under boundary conditions of the third kind:

$$\Phi_r = \frac{\mathrm{T_m} - T_{\mathrm{air}}}{\frac{1}{\alpha_{emit}\cdot S_{l.m}} + \frac{\delta_\mathrm{r}}{\lambda_\mathrm{r}\cdot S_{\mathrm{p}.r}} + \frac{1}{\alpha_{\mathrm{c.t.h}}\cdot S_{\mathrm{t.h}}}}\cdot 10^{-3} \quad (5)$$

4. Heat loss through the "collar":

The power of heat loss through the lining of the "collar" is calculated according to the formula of complex heat transfer under boundary conditions of the third kind:

$$\Phi_v = \frac{\mathrm{T_m} - T_{\mathrm{air}}}{\frac{1}{\alpha_{emit}\cdot S_{l.m}} + \frac{\delta_{\mathrm{n.l}}}{\lambda_{\mathrm{n.l}}\cdot S_{\mathrm{p}.n.l}} + \frac{\delta_{\mathrm{con}}}{\lambda_{\mathrm{con}}\cdot S_{\mathrm{p}.con}} + \frac{1}{\alpha_{\mathrm{c.t.h}}\cdot S_{\mathrm{t.h}}}}\cdot 10^{-3} \quad (6)$$

where $S_{x.y}$ – Areas of heat-releasing surfaces of concrete layers, stuffed layers, as well as the area of the heat-receiving surfaces of different layers are calculated on the basis of geometric formulas, taking into account the linear values of the crucible of ICF-6 factory basis.

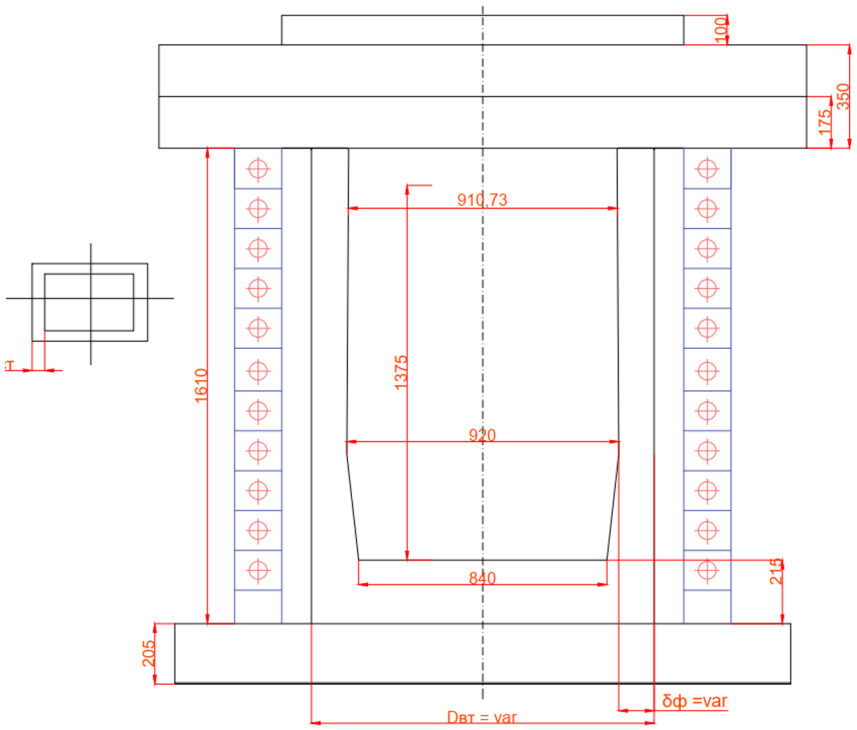

Fig. 2. Scheme of thermal circuits

3 Results and their discussion

The power of heat loss through the lining of the furnace is determined on the basis of complex heat transfer formulas under boundary conditions of the first and third kind (3 – 6), taking into account the following data:

For heat loss through wall lining (for dealing he equation-3).

The temperature of the liquid metal in the crucible $T_m = 1900\ K$;

$T_{H_2O} = 300\ K$ - the temperature of the water cooling the inductor;

$\lambda_l = 2.1\ W/(m \cdot K)$ - thermal conductivity of the printed mass at;

$T_{cp} = (T_p + T_{H_2O})/2 \approx 1100\ K$

$h_m = 1.350\ m$ – the depth of the metal (see Fig. 2);

$D_m = 920\ mm = 0.92\ m$ – the inner diameter of the crucible (see Fig. 2);

$d_{l.m} = 6.7\ t/m^3$ – density of liquid steel grade 20GL;

$D_{vт} = D_m + 2\delta_l = variable\ (var)$ – the outer diameter of the crucible, equal to the inner diameter of the inductor with a variable thickness of the wall of the crucible lining mm; $\delta_l = 100, 110, 120, 130, 140\ and\ 150$

$\delta_c = 5\ mm = 0.005\ m$ – thickness of electrical insulating coating;

$\lambda_c = 0.7\ Wt/(m \cdot K)$ – thermal conductivity of the protective coating of the inductor at medium temperature; $T_{cp} \approx 1100\ K$

$S_{p.c} = \pi D_{vт} h_i = var$ - estimated area of coating with a thickness of 0.005 m;

$h_i = 1630\ mm = 1.63\ m$ – the height of the inductor (see Fig. 2);

$\lambda_{ст} = 384\ W/(m \cdot K)$ – thermal conductivity of copper at T=320 *K*.

$\alpha_{c.t.h} = 5000\ W/(m^2 \cdot K)$ – coefficient of convective heat transfer in the water cooling system of the inductor;
$S_{c.t.h} = \pi D_{vт} h_i = var$ - the area of the heat-dissipating surface of the inductor.
δ_w Rational (taking into account electromagnetic phenomena) wall thickness of the ICF-6 with a frequency is calculated according to the formula: $f = 500\ Hz$

$$\delta_{\text{w}} = \frac{\pi}{2}\delta_{\text{i}} = \frac{\pi}{2} \cdot 500 \cdot \sqrt{\frac{\rho_i}{\mu_r f}} = \frac{\pi}{2} \cdot 500 \cdot \sqrt{\frac{2 \cdot 10^{-8}}{1 \cdot 500}} = 5\ mm = 0.005\ m$$

where is the specific electrical resistance of the water-cooled copper inductor; $\rho_i = 2 \cdot 10^{-8}\ Ohm \cdot m$; $\mu_r = 1$ – relative magnetic permeability for a diamagnetic copper inductor; $S_{\text{p.w}} \approx \pi D_{vт} h_i = var$ is the calculated wall area of the inductor at the wall thickness. $\delta_{\text{ст}} = 0.005\ m$.

For heat loss through the bottom lining (for dealing he equation-4)

$T_{\text{air}} = 295\ K$ – ambient temperature;
$\delta_{\text{lay}} = 215\ mm = 0{,}215\ m$ – the thickness of the padded periclase layer;
$\lambda_{\text{lay}} = 1.9\ W/(m \cdot K)$ - thermal conductivity of the stuffing layer at
$T_{aver} = \frac{1900+1000}{2} = 1450\ K$;
$S_{lay} = var$ calculated area of the stuffing layer, m^2;
$\delta_{\text{con}} = 200\ mm = 0{,}2\ m$ – concrete layer thickness;
$\lambda_{\text{con}} = 0{,}68\ W/(m \cdot K)$ – thermal conductivity of refractory concrete with chamotte filler at $T_{aver} = 500\ K$;
$S_{\text{p.con}}$ – calculated area of the concrete layer, m^2.
$\alpha_{\text{c.t.h.}} = 16.11 \cdot 0{,}7 = 11.28\ \frac{Wt}{m^2 \cdot K}$ - coefficient of convective heat transfer from the heat-releasing surface, facing down at $T_{sur} \approx 400\ K$;

For heat loss through the roof (for dealing he equation-5).

$S_{l.m}$ - heat-releasing surface area of liquid metal;
$\delta_{\text{r}} = 140\ mm = 0.14\ m$ - roof lining thickness;
$\lambda_{\text{r}} = 2.87\ W/(m \cdot K)$ – thermal conductivity of the periclase-chromite dome at $T_{aver} = 1000\ K$;
$\alpha_{\text{c.t.h}} = 16.11 \cdot 1.3 = 21\ \frac{W}{m^2 \cdot K}$ - coefficient of convective heat transfer from the heat-releasing surface of the roof, facing upward at $T_r \approx 400$ K;
$\alpha_{\text{emit}} = \frac{\varepsilon_{\text{пр}} \cdot \sigma_0 \cdot (\text{T}_\text{m}^4 - \text{T}_\text{r}^4)}{\text{T}_\text{m} - \text{T}_\text{r}}$ - coefficient of heat transfer by radiation according to the Stefan-Boltzmann law, formally described according to the Newton-Richmann law for convective heat transfer through the temperature difference to the first power (temperature difference);
$\sigma_0 = 5.67 \cdot 10^{-8}\ \frac{Wt}{m^2 \cdot K^4}$ - Stefan-Boltzmann constant;
$\text{T}_r = 1500\ K$ - temperature of the heat-receiving roof surface;
$\varepsilon_{corr} = \left[\frac{1}{\varepsilon_{l.m}} + (\frac{1}{\varepsilon_l} - 1) \cdot \chi_{l-m}\right]^{-1}$ – reduced emissivity;
$\varepsilon_{l.m}$ and ε_l – the degree of blackness of the "gray" surfaces of liquid metal (taken at T=1900 K $\varepsilon_{l.m}$=0.60) and linings (ε_l=0.80);
$\chi_{\text{l-m}}$ - angular coefficient determined by the ratio of the surface areas of the liquid metal and the heat-receiving surface of the ICF-6 lining in the form $\chi_{\text{l-m}} = \frac{\text{S}_{\text{l.m}}}{\text{S}_{\text{l}}}$ taking into account the aperture factor;

$$\chi_{l-m} = \frac{S_{l.m}}{S_l} = \frac{\frac{\pi \cdot D_m^2}{4}}{\pi \cdot D_m \cdot \delta_r + \frac{\pi \cdot D_r^2}{4}} = \frac{D_m}{4 \cdot (\delta_r + \frac{D_r}{4})} = \frac{1{,}05}{\frac{4 \cdot 0.24}{1.05} + 1} = 0.652;$$

$$\varepsilon_{corr} = \left[\frac{1}{0.60} + (\frac{1}{0.80} - 1) \cdot 0.522\right]^{-1} = 0.547;$$

$$\alpha_{emit} = \frac{0{,}547 \cdot 5{,}67 \cdot 10^{-8} \cdot (1900^4 - 1500^4)}{1900 - 1500} \approx 617.42 \ \frac{W}{m^2 \cdot K}.$$

For heat loss through the "collar" (for dealing he equation-6)

$\delta_{col} = 300\ mm = 0{,}30\ m$ - collar lining thickness;

$\alpha_{emit} = \frac{\varepsilon_{cor} \cdot \sigma_0 \cdot (T_m^4 - T_{h.r}^4)}{T_m - T_{h.r}}$ - coefficient of heat transfer by radiation according to the Stefan-Boltzmann law, formally described according to the Newton-Richmann law for convective heat transfer through the temperature difference to the first power (temperature difference);

$T_{h.r} = 1500\ K$ - temperature of the heat-receiving surface of the "collar";

$\varepsilon_{cor} = \left[\frac{1}{\varepsilon_{l.m}} + (\frac{1}{\varepsilon_l} - 1) \cdot \chi_{l-m}\right]^{-1}$ – reduced emissivity;

$\varepsilon_{l.m}$ and ε_l – the degree of blackness of the "gray" surfaces of liquid metal (taken at T=1900K $\varepsilon_{l.m}$=0.60) and linings (ε_l=0.80);

$$\chi_{l-m} = \frac{S_{l.m}}{S_l} = \frac{\frac{\pi \cdot D_m^2}{4}}{\pi \cdot D_m \cdot \delta_v + \frac{\pi \cdot D_v^2}{4}} = \frac{D_m}{4 \cdot (\delta_v + \frac{D_v}{4})} = \frac{1{,}05}{4(0{,}3 + \frac{1{,}05}{4})} = 0.434;$$

$$\varepsilon_{cor} = \left[\frac{1}{0.60} + (\frac{1}{0.58} - 1) \cdot 0.467\right]^{-1} = 0.505;$$

$$\alpha_{emit} = \frac{0.505 \cdot 5.67 \cdot 10^{-8} \cdot (1900^4 - 1500^4)}{1900 - 1500} \approx 570.3 \ \frac{W}{m^2 \cdot K};$$

$\delta_{n.l} = var$ – thickness of the printed periclase layer;

$\lambda_{n.l} = 1.9\ W/(m \cdot K)$ - thermal conductivity of the stuffing layer at $T_{aver} = \frac{1900+1000}{2} \approx 1450\ K$;

$S_{p.l}$ – calculated area of the padding layer of the "collar", m^2;

$\delta_{con.v} = 500\ mm = 0.50\ m$ – thickness of the concrete layer of the "collar";

$\lambda_{бет} = 0.68\ W/(m \cdot K)$ – thermal conductivity of heat-resistant concrete with fireclay filler at $T_{aver} = 500\ K$;

$S_{p.con}$ – estimated area of the concrete layer "collar", m^2;

$\alpha_{c.t.h} = 16.11\ \frac{W}{m^2 \cdot K}$ - coefficient of convective heat transfer from the heat-releasing surface of the "collar", at $T_v \approx 400$ K;

$S_{t.h} = \pi D_v \delta_v + \frac{\pi}{2}(D_v^2 - D_{vr}^2) = var$ - the area of the heat-releasing surface of the "collar".

Total heat loss

The results of calculating the total heat losses for different thicknesses of the ICF-6 crucible lining are shown in Table 3 and Fig. 3.

Table 3. Total heat losses of ICF-6

δ_l,m	0.1	0.11	0.12	0.13	0.14	0.15
$P_{h.l}$, kWt	145.9	136.6	128.8	122.1	116.3	111.3

Active power lost in the inductor

The active power lost in the inductor is calculated by the formula

$$P_i \approx 6.2 \cdot 10^{-6} (IN_1)^2 D_{vT} h_i \sqrt{\rho_i f} \frac{k_{I.P}}{k_з} = var,$$

where $IN_1 = 10^5$ A/m - inductor current flooring, which determines the magnitude of the magnetic field strength on the inner surface and in the cavity of the inductor; $k_з = 0.72$ – inductor fill factor, (at N=14, inductor winding pitch 125 mm and pipe height 90 mm).

The results of calculating the active power lost in the inductor with different thicknesses of the ICF-6 lining are shown in Table 4 and Fig. 3.

Table 4. Active power lost in the inductor

δ_l, **m**	0.1	0.11	0.12	0.13	0.14	0.15
P_i, **kW**	497.1	506.0	514.9	523.8	532.6	541.5

Determination of the power released in the metal

Useful power at $\tau_{smelt} = 38$ min and specific useful energy is determined by the formula

$$W_{y.т} = 343 \text{ kW} \cdot \text{h/t}$$

Useful power at and specific useful energy is determined by the formula

$$P_{sum} = \frac{W_{y.т} m_0}{\tau_{smelt}} = \frac{343 \cdot 6 \cdot 60}{38} = 3250\ kW.$$

The power released in the metal is:

$$P_m = P_{sum} + P_{h.l} = var \text{ (tab.5).}$$

Table 5. Power released in the metal

$\boldsymbol{\delta_l}$**,m**	0.1	0.11	0.12	0.13	0.14	0.15
$\boldsymbol{P_m}$**, kW**	3395.5	3386.3	3378.4	3371.7	3365.9	3360.8

Thermal efficiency equals:

$$\eta_{\text{th.ef}} = \frac{P_{\text{sum}}}{P_{\text{m}}} = \frac{P_{\text{sum}}}{P_{\text{sum}} + P_{\text{h.l}}} = var \text{ (tab. 6, fig.4).}$$

Electrical efficiency equals:

$$\eta_{\text{el.ef}} = \frac{P_{\text{m}}}{P_{\text{m}} + P_{\text{i}}} = var \text{ (tab. 6, fig.4).}$$

Overall efficiency equals:

$$\eta_o = \eta_{th.ef} \cdot \eta_{el.ef} = \frac{P_{sum}}{P_m + P_i} = 1 - \frac{P_i + P_{h.l}}{P_m + P_i} = var \text{ (tab. 6, fig.4).}$$

Table 6. Efficiency with different lining thicknesses

δ_l,m	0.1	0.11	0.12	0.13	0.14	0.15
$\eta_{th.ef}$	97.1	97.2	97.4	97.5	97.6	97.7
$\eta_{th.ef}$	90.9	90.8	90.6	90.4	90.3	90.1
η_o	88.3	88.3	88.2	88.2	88.2	88.1

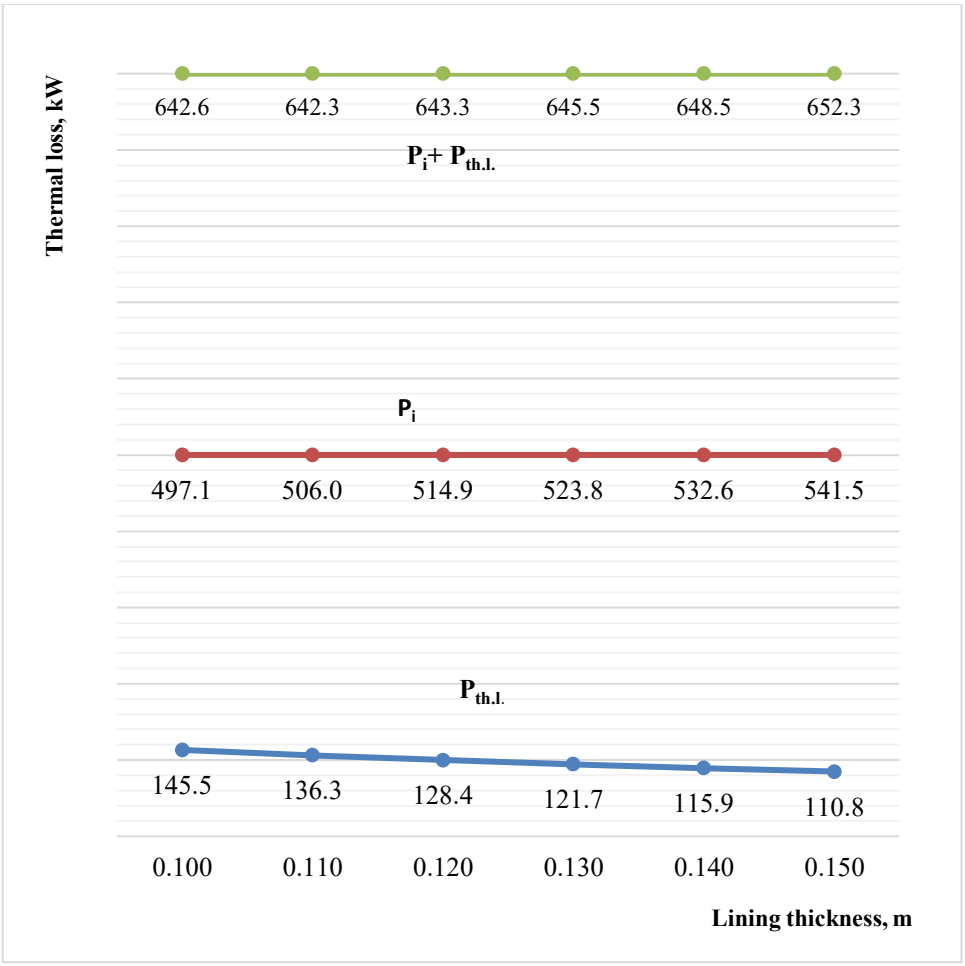

Fig. 3. Active power lost in the inductor with different thicknesses of the ICF-6 lining

Fig. 4. Change in the performance of the ICF-6 depending on the thickness of the lining of the LMZ crucible

4 Conclusions

On the basis of thermal and electrical calculations for ICF-6 LMZ with a capacity of 6 tons, the rational thickness of the lining of the crucible wall is equal to $\delta_l = 0.115 \ldots 0.120\, mm$, which corresponds to the relation $\frac{D_{vr}}{D_m} = 1.23 \ldots 1.26$.

These calculations make it possible to optimize the thickness of the lining, taking into account the thermodynamic and thermal processes taking place in the liquid metal bath and on the boundaries of the refractory layer of the lining. In the future, the rational thickness of the lining around the crucible will reduce heat loss to the environment and increase the energy efficiency of the furnace.

References

1. Muratovich T. T., Kayumjonovich T. N., Pirmukhamedovich A. S., and Teleubaevich U. T. Selection of the material of the lining of induction furnaces in steel 20GL. Web of Scientist: International Scientific Research Journal, Vol. 3(5), pp.1728-1739. (2022).
2. Muratjonovich T. T., Tileubaevich U. T., Nikolayevna A. A., Islomovna N. D., and Ibroximovich M. S. Magnetic field of a real inductor of induction furnaces. Web of Scientist: International Scientific Research Journal, Vol. 3(6), pp. 842-849. (2022).
3. Muratovich T. T., Kayumjonovich T. N., Tileubaevich U. T., and Pirmukhamedovich, A. S. Study of electromagnetic phenomena and its main parameters in the crucible of induction furnaces during smelting steel 20GL. Web of Scientist: International Scientific Research Journal, Vol. 3(6), pp.85-95. (2022).
4. Muratjonovich T. T., Tileubaevich U. T., Nikolayevna A. A., Islomovna N. D., and Ibroximovich M. S. Magnetic field of a real inductor of induction furnaces. Web of Scientist: International Scientific Research Journal, Vol. 3(6), pp.842-849. (2022).
5. Tursunov N. K., Semin A. E., and Sanokulov E. A. Study of desulfurization process of structural steel using solid slag mixtures and rare earth metals. Chernye metally, Vol. 4, pp.32-37. (2016).
6. Tursunov N. K., Semin A. E., Kotelnikov G. I. Kinetic features of desulphurization process during steel melting in induction crucible furnace. *Chernye Metally*. Vol. 5. pp.23-29. (2017).
7. Toirov O., and Tursunov N. Development of production technology of rolling stock cast parts. In E3S Web of Conferences, Vol. 264, p. 05013. (2021).
8. Tursunov N. K., Semin A. E., and Sanokulov E. A. Study of dephosphoration and desulphurization processes in the smelting of 20GL steel in the induction crucible furnace with consequent ladle treatment using rare earth metals. Chernye Metally, Vol.1, pp. 33-40. (2017).
9. Toirov O., Tursunov N., Alimukhamedov S., and Kuchkorov L. Improvement of the out-of-furnace steel treatment technology for improving its mechanical properties. In E3S Web of Conferences, Vol. 365, p. 05002. (2023).
10. Kuchkorov L., Alimukhamedov S., Tursunov N., and Toirov O. Effect of different additives on the physical and mechanical properties of liquid-glass core mixtures. In E3S Web of Conferences, Vol. 365, p. 05009. (2023).
11. Turakulov M., Tursunov N., and Alimukhamedov S. Development of technology for manufacturing molding and core mixtures for obtaining synthetic cast iron. In E3S Web of Conferences, Vol. 365, p. 05006. (2023).

12. Yunusov S., Sultonov A., Rakhmatov M., Bobomurotov T., and Agzamov M. Results of studies on extending the time operation of gin and linter grates. In E3S Web of Conferences, Vol. 304, p. 03028. (2021).
13. Dzhuraev A., Yunusov S., Mirzaumidov A., Umarov K., and Matkarimov A. Development of an effective design and calculation for the bending of a gin saw cylinder. International journal of advanced science and technology, Vol. 29(4), pp.1371-1390. (2020).
14. Agzamov M. M., Yunusov S. Z., and Gafurov J. K. On the technological development of cotton primary processing, using a new drying-purifying unit. In IOP Conference Series: Materials Science and Engineering, Vol. 254, No. 8, p. 082017. (2017).
15. Makhkamov N. Y., Yusupov G. U., Tursunov T., and Djalilov K. Properties of metal-based and nonmetal-based composite materials: A brief review. In IOP Conference Series: Earth and Environmental Science, Vol. 614, No. 1, p. 012068. (2020).
16. Radkevich M., Pulatova T., Shipilova K., Pochuzhevsky O., Gapirov A., and Turakulov M. Possibilities of using lianas for greening automobile roads. (2021).
17. Kasimov O., Fayzibayev, S., Djanikulov, A., and Mamayev, S. Numerical studies for estimation of temperature fields in bandage material during locomotive braking. In AIP Conference Proceedings, Vol. 2432, No. 1, p. 030025. (2022).
18. Ryskulov A. A., Liopo V. A., Ovchinnikov E. V., and Eisymont E. I. Phase transformations in tribosystems with metal-polymer components. Journal of Friction and Wear, Vol. 32(1), pp.30-36. (2011).
19. Nurkulov F., Ziyamukhamedova U., Rakhmatov E., and Nafasov J. Slowing down the corrosion of metal structures using polymeric materials. In E3S Web of Conferences, Vol. 264, p. 02055. (2021).
20. Ibadullaev A., Teshabayeva E., Kakharov B., and Babaev A. Elastomeric materials based on new ingredients. In AIP Conference Proceedings, Vol. 2432, No. 1, p. 030021. (2022).
21. Ibadullaev A., Nigmatova D., and Teshabaeva E. Radiation Resistance of Filled Elastomer Compositions. In IOP Conference Series: Earth and Environmental Science, Vol. 808, No. 1, p. 012043. (2021).
22. Ibadullayev A., Teshabayeva E., Kakharov B., and Nigmatova D. Composite elastomeric materials filled with modified mineral fillers. In E3S Web of Conferences, Vol. 264, p. 05006. (2021).
23. Ibadullaev A., Yusupbekov A. K., Gorbunov V. A., and Abdurashidov T. R. Reactivity of a secondary carbonaceous raw-material with respect to carbon-dioxide. Journal of applied chemistry of the USSR, Vol. 59(11), pp. 2387-2389. (1986).